

The role of astrocytic calcium and TRPV4 channels in neurovascular coupling

Allanah Kenny¹ · Michael J. Plank² · Tim David¹

Received: / Accepted:

Abstract Neuronal activity evokes a localised change in cerebral blood flow in a response known as neurovascular coupling (NVC). Although NVC has been widely studied the exact mechanisms that mediate this response remain unclear; in particular the role of astrocytic calcium is controversial.

Mathematical modelling can be a useful tool for investigating the contribution of various signalling pathways towards NVC and for analysing the underlying cellular mechanisms. The lumped parameter model of a neurovascular unit with both potassium and nitric oxide (NO) signalling pathways and comprised of neurons, astrocytes, and vascular cells has been extended to include the glutamate induced astrocytic calcium pathway with EET signalling and the stretch dependent TRPV4 calcium channel on the astrocytic endfoot.

Results show that the potassium pathway governs the fast onset of vasodilation while the NO pathway has a delayed response, maintaining dilation longer following neuronal stimulation. Increases in astrocytic calcium concentration via the calcium signalling pathway and/or TRPV4 channel to levels consistent with experimental data are insufficient for inducing either vasodilation or constriction, in contrast to a number of experimental results. It is shown that the astrocyte must depolarise in order to produce a significant potassium flux through the astrocytic BK channel. However astrocytic calcium is shown to strengthen potassium induced

NVC by opening the BK channel further, consequently allowing more potassium into the perivascular space. The overall effect is vasodilation with a higher maximal vessel radius.

Keywords neurovascular coupling · mathematical modelling · astrocytic calcium · TRP channel · large-conductance calcium-sensitive potassium channel

1 Introduction

The cerebral cortex contains a multitude of blood vessels that regulate blood supply in response to local changes in a process known as functional hyperaemia. This process is characterised by an increase in neuronal activity followed by a rapid dilation of local blood vessels and hence increased blood supply providing oxygen and glucose necessary for cellular function. Impaired functional hyperaemia resulting in reduced blood supply to brain tissue is associated with several neurological disorders such as migraine, subarachnoid and intracranial haemorrhage, Alzheimers disease, and cortical spreading depression (CSD) (Bogdanov et al. 2016; Pietrobon and Moskowitz 2014; Lauritzen et al. 2011; Girouard and Iadecola 2006).

Functional hyperaemia is controlled through the process of neurovascular coupling (NVC). This process involves an intercellular communication system based on ion exchange through pumps and channels between neurons, astrocytes (glial cells), smooth muscle cells (SMCs), endothelial cells (ECs), and the small spaces between these cells: the synaptic cleft (SC) between the neuron and astrocyte, and the perivascular space (PVS) between the astrocyte and SMC (Drewes

Allanah Kenny
E-mail: allanah.kenny@pg.canterbury.ac.nz

¹ High Performance Computing Centre, University of Canterbury, New Zealand

² Department of Mathematics and Statistics, University of Canterbury, New Zealand

2012; Attwell et al. 2010; Hamel 2006; Iadecola 2004). Together these communicating cells comprise a neurovascular unit (NVU).

There has been significant work done on the vascular response to neuronal activity and astrocytic inputs (Bennett et al. 2008a; Filosa et al. 2004; Farr and David 2011; Dormanns et al. 2014) but little has been done to investigate the effect that the vasculature has on astrocytes. Moore and Cao (2008) hypothesised that the cerebral vasculature has an important effect on neural function through various mechanisms. Witthoft and Karniadakis (2012) suggested that one indirect mechanism is through astrocytic mechanosensation of vascular motions. Their bidirectional signalling model includes the astrocyte response to vascular function via the transient receptor potential vanilloid-related 4 (TRPV4) channel, a mechanosensitive calcium (Ca^{2+}) channel on the astrocytic endfoot (Benfenati et al. 2007). The model was validated using experimental data from Cao (2011) who provided evidence that vessel dilation provokes astrocytic Ca^{2+} increase and membrane depolarisation. Dunn et al. (2013) have also shown that TRPV4-mediated Ca^{2+} influx contributes to the astrocytic endfoot response to neuronal activation, enhancing vasodilation.

There is some debate as to the importance of astrocytic Ca^{2+} towards NVC (Bazargani and Attwell 2016). Zonta et al. (2003) observed experimentally that glutamate activated astrocytic endfoot Ca^{2+} increases were well-timed with vascular changes; these observations were the first evidence that astrocytes may contribute towards NVC. An increase in astrocytic Ca^{2+} can result in the production of arachidonic acid (AA) which is subsequently metabolised to epoxyeicosatrienoic acids (EETs) and prostaglandin E₂ (PgE₂), a derivative of cyclooxygenase enzymes (COX) (Cahoy et al. 2008). These metabolites may act directly on SMCs (Attwell et al. 2010) or directly on the astrocytic endfeet to modulate potassium (K^+) currents Higashimori et al. (2010). Numerous *in vivo* experimental results (Nizar et al. 2013; Bonder and McCarthy 2014; Takata et al. 2013) indicate that NVC can occur independently of large astrocytic Ca^{2+} signalling. Whereas various *in situ* experimental results (Filosa et al. 2006; Straub et al. 2006; Girouard et al. 2010) support the hypothesis that astrocytic endfoot Ca^{2+} is a critical factor for NVC. In particular, Girouard et al. (2010) examined the effect of astrocytic Ca^{2+} on the vascular response with brain slices. The Ca^{2+} concentration was elevated by either electro field stimulation (EFS) or by uncaging Ca^{2+} in the astrocytic endfeet. They found that, regardless of the

elevation method, moderate increases in Ca^{2+} concentration resulted in vasodilation while large increases resulted in constriction (see Figure 1).

It is unclear whether *in situ* or *in vitro* experiments are representative of physiology; using a numerical model “*in silico*” allows for a different approach. These *in silico* simulations can be a useful tool for guiding future experiments and providing a deeper understanding of physiological processes. Mathematical modelling provides a number of key benefits, in particular the ability to measure quantities and isolate signalling pathways that are difficult or impossible to implement in a wet lab environment.

A mathematical model of a single NVU has been presented in the work of Dormanns et al. (2016) based on the previous model of Dormanns et al. (2014). This model describes the synaptic K^+ induced NVC pathway, where synaptic K^+ is taken up by the astrocyte and extruded into the PVS, culminating in vasodilation via the relaxation of the SMC. This K^+ induced NVC pathway is implemented in conjunction with nitric oxide (NO) dynamics. NO is a neurotransmitter primarily produced in both the neuron and EC and able to diffuse into the SMC where it acts as a potent cerebral vasodilator.

We present here an extension to the mathematical model of Dormanns et al. (2016). The model has been extended to include glutamate mediated astrocytic Ca^{2+} dynamics, the subsequent production of EETs, and their combined effect on the big potassium (BK) channel on the astrocytic endfoot. We assume that the EETs do not diffuse through the PVS to the arteriole, but act primarily upon the astrocytic BK channel. It is possible that EETs or other AA-derived metabolites act on the SMCs themselves Attwell et al. (2010), but we assume, in keeping with the findings of Higashimori et al. (2010), that EETs act directly upon the astrocytic endfoot. Our model does not yet include the COX - PgE₂ pathway, although findings from Metea and Newman (2006) suggest that it is EETs rather than PgE₂ that result in vasodilation.

The model has been extended to also include a stretch dependent TRPV4 channel on the astrocytic endfoot based on the model of Witthoft and Karniadakis (2012), allowing for the direct study of the influence of this bidirectional coupling of the astrocyte and vasculature. The relative efficacy of these different pathways on the process of NVC can be examined using our complex and more comprehensive NVU model. The final extension to the model is an extracellular

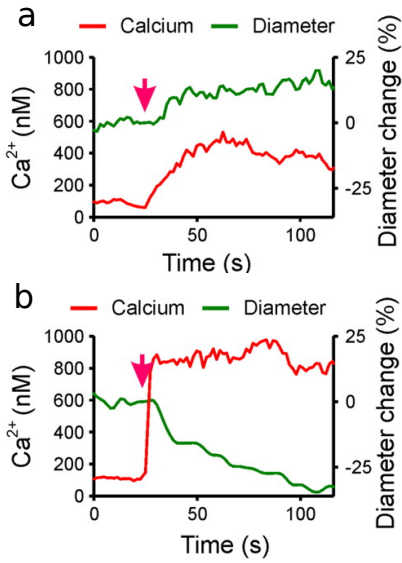


Fig. 1: Experimental *in situ* results of Girouard et al. (2010) show that a) moderate increases in Ca^{2+} concentration in the astrocytic endfoot up to $0.324 \pm 0.016 \mu\text{M}$ results in vasodilation, whereas b) high Ca^{2+} levels of $0.732 \pm 0.041 \mu\text{M}$ result in vasoconstriction.

Adapted from Girouard et al. (2010).

space (ECS) compartment, however this is not the focus of this paper and as such is not discussed in great detail.

The paper is laid out as follows. An overview of the foundation NVU model by Dormanns et al. (2016) containing K^+ and NO dynamics is found in Section 2. Section 3 describes the various extensions to the model: astrocytic Ca^{2+} dynamics, the TRPV4 channel, and the ECS compartment. Section 4 contains the results where we primarily examine the influence of astrocytic Ca^{2+} and the TRPV4 channel on NVC. Finally Section 5 contains a discussion of these results and the limitations and future direction of our research.

2 Foundation model

The foundation NVU model is based on the work of Dormanns et al. (2014, 2016) and is comprised of 7 compartments: neuron, SC, astrocyte, PVS, SMC, EC, and the lumen. A schematic representation of the proposed model encompassing the following pathways is found in Figure 2 for reference.

During neuronal stimulation both K^+ and glutamate are released from the neuron into the SC. This K^+ release is sim-

ulated by an input function $K(t)$ which has the temporal form of a beta distribution as follows.

For $t_0 \leq t \leq t_0 + \Delta t$:

$$K(t) = K_{in} \frac{(\alpha + \beta - 1)!}{(\alpha - 1)!(\beta - 1)!} \left(\frac{t_\beta - (t - t_0)}{\Delta t} \right)^{\beta-1} \left(\frac{t - t_0}{\Delta t} \right)^{\alpha-1} \quad (1)$$

For $t_1 \leq t \leq t_1 + \Delta t$:

$$K(t) = -K_{in} \quad (2)$$

Otherwise:

$$K(t) = 0 \quad (3)$$

where K_{in} is a scaling factor, t_0 and t_1 are the start and end times of neuronal stimulation respectively, α_n , β_n and t_β are beta distribution constants, and Δt is the initial input duration. The beta distribution form ensures that the K^+ flux from the neuron into the SC at t_0 is equal to the amount taken back by the neuron at t_1 . This function is added to the ordinary differential equation (ODE) for synaptic K^+ concentration (see Dormanns et al. (2014) for further details).

The glutamate concentration in the SC is described by the input function $\text{Glu}(t)$ as given by

$$\text{Glu}(t) = \text{Glu}_{\max} \left[0.5 \tanh \left(\frac{t - t_0}{\theta_L} \right) - 0.5 \tanh \left(\frac{t - t_1}{\theta_R} \right) \right] \quad (4)$$

where Glu_{\max} is the maximum glutamate concentration corresponding to the release of one vesicle, and θ_L , θ_R are slope scaling factors. The glutamate concentration is used in the equations for the fraction of open N-methyl-D-aspartate (NMDA) receptors (see Dormanns et al. (2016) for further details). These parameters can be found in Table 1 in the Appendix.

2.1 K^+ pathway

During neuronal stimulation K^+ is released into the SC, leading to an influx of K^+ into the astrocyte via sodium potassium pumps on astrocytic processes adjacent to the SC. Consequently the astrocyte depolarises, leading to a large K^+ efflux into the PVS through the BK channel on the astrocytic endfoot (Chung et al. 2007).

The rise in perivascular K^+ concentration leads to a further influx of K^+ through the inward rectifying K^+ (KIR) channel from the SMC into the PVS, hyperpolarising the SMC membrane. As a result the voltage operated Ca^{2+} channels

(VOCCs) on the SMC close, preventing an influx of Ca^{2+} . The decrease in Ca^{2+} concentration causes a decrease in the rate constants K_1 and K_6 for the phosphorylation of free and attached cross bridges, respectively. Overall the change in the actin-myosin cross bridge formation relaxes the SMC, dilating the vessel which results in increased blood flow. This K^+ induced NVC pathway is well known (Attwell et al. 2010; Filosa et al. 2006; Nakahata et al. 2006).

2.2 NO pathway

NO is a neurotransmitter known to act as a potent cerebral vasodilator. The biochemical reaction that synthesises NO is catalysed by the enzyme family of NO synthases (NOS): neuronal (nNOS), endothelial (eNOS), and inducible (iNOS), found in neurons, ECs and multiple cell types respectively (Förstermann 2006). The production rate of NO is dependent on the concentration of activated NOS. nNOS and eNOS are thought to be the most influential NO producers, hence it is assumed NO production is in only the neuron and EC compartments and no production in the other cell types. However NO is able to diffuse rapidly into other compartments.

NO production in the EC is catalysed by eNOS and mediated by wall shear stress (WSS) and endothelial Ca^{2+} concentration, where WSS is dependent on the radius. Endothelial NO is produced continuously and independent of neuronal activity. During neuronal stimulation, glutamate is released into the SC, inducing a Ca^{2+} influx into the neuron through NMDA receptor channels. The Ca^{2+} binds with calmodulin to form calmodulin/calcium (CaM) complexes, which act to increase nNOS production and hence increase neuronal NO production.

When NO diffuses into the SMC it interacts with intracellular enzyme activation and regulates SMC relaxation as follows. NO activates soluble guanylyl cyclase (sGC) by increasing the constants k_1 and k_3 , where k_1 is the reaction rate from sGC in the basal state (E_b) to the intermediate form (E_{6c}), and k_3 is the reaction rate from the intermediate to fully activated form (E_{5c}). Activated sGC catalyses the formation of cyclic guanosine monophosphate (cGMP), which increases the rate constants K_2 and K_5 for the dephosphorylation of free and attached cross bridges, respectively. cGMP also acts to open the BK channel so that both the SMC K^+ concentration and membrane potential decrease, closing the VOCC channel. As a result the SMC Ca^{2+} concentration decreases and the rate constants K_1 and K_6 also

decrease. Overall the addition of the NO pathway to the model has a vasodilatory effect.

3 Model extensions

This section details the extensions to the single NVU model, in particular the addition of the astrocytic Ca^{2+} pathway, TRPV4 channel, and the extracellular space compartment. The following equations form an extension to the foundation NVU model of Dormanns et al. (2016) and Dormanns et al. (2014) where the remaining equations are detailed. A schematic diagram of the proposed model containing the various extensions is found in Figure 2 for reference.

3.1 Astrocytic Ca^{2+} pathway

The first extension to the NVU model is of the astrocytic Ca^{2+} pathway and based on the model of Farr and David (2011). The release of glutamate in the SC induces an inositol trisphosphate (IP_3) release into the astrocyte, causing the release of calcium from the endoplasmic reticulum (ER) into the cytosol, which in turn leads to the production of EETs. The membrane potential, EET concentration and Ca^{2+} concentration regulate the opening of the BK channel, allowing further K^+ release into the PVS.

The ratio ρ of bound to unbound metabotropic receptors on the astrocytic process adjacent to the SC is dependent on the synaptic glutamate release according to the following relation:

$$\rho = \rho_{\min} + \frac{\rho_{\max} - \rho_{\min}}{Glu_{\max}} Glu(t) \quad (5)$$

where $Glu(t)$ is the smooth pulse function in Equation (4). The ratio G of active to total G-protein due to metabotropic glutamate receptor (mGluR) binding on the astrocyte end-foot surround the SC is then given by

$$G = \frac{\rho + \delta}{K_G + \rho + \delta} \quad (6)$$

where K_G is the G-protein disassociation constant and δ is the ratio of the activities of the bound and unbound receptors, which allows for background activity in the absence of any stimulus (Bennett et al. 2008b). The glutamate attachment at metabotropic receptors induces an increase in astrocytic IP_3 concentration i_k according to the following ODE:

$$\frac{di_k}{dt} = r_h G - k_{deg} i_k \quad (7)$$

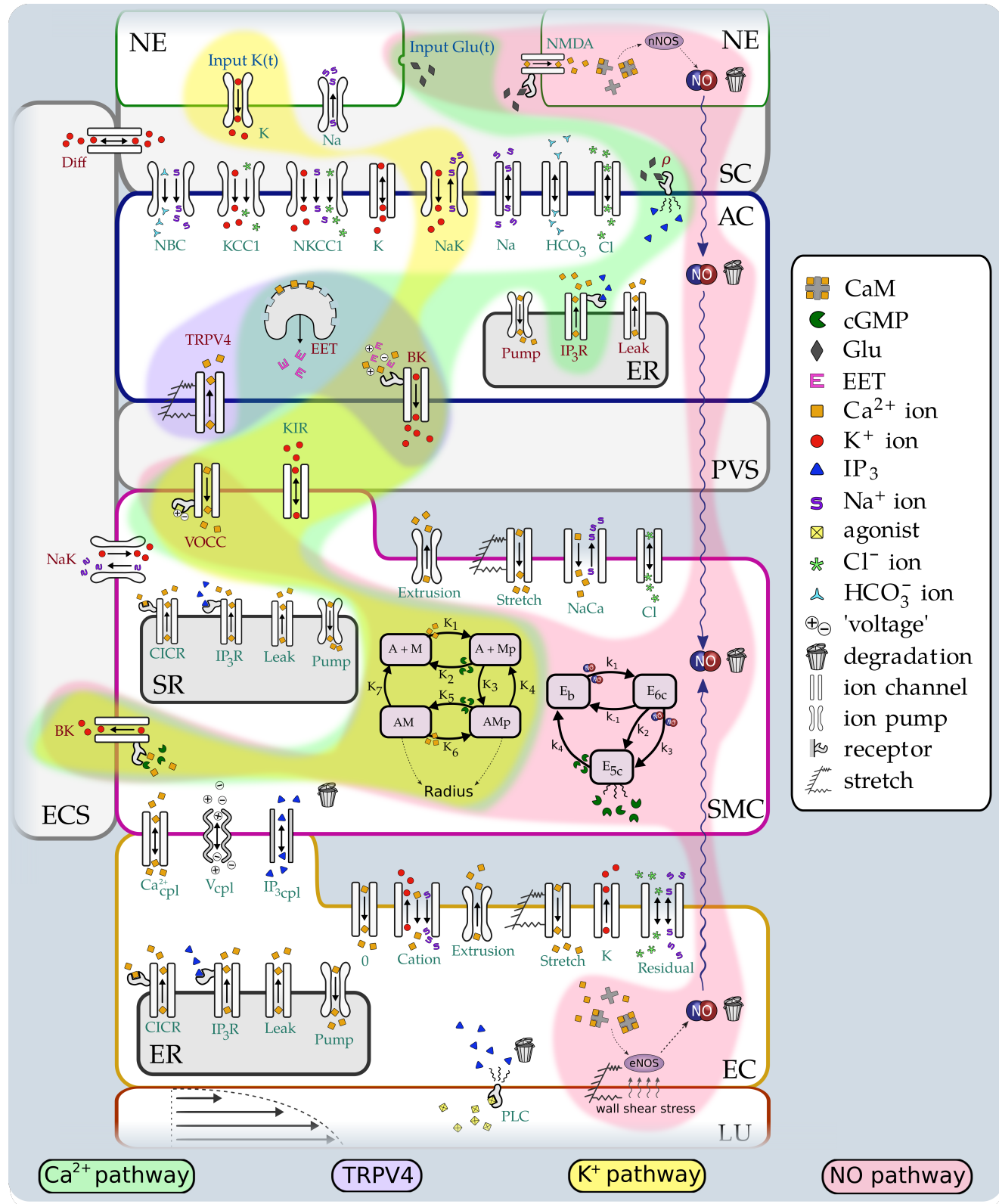


Fig. 2: A schematic representation of the proposed NVC model with added astrocytic Ca^{2+} pathway (green), TRPV4 channel (purple) and extracellular space compartment. Channels or pumps that have been added or modified are labelled in red. NE: neuron, SC: synaptic cleft, AC: astrocyte, PVS: perivascular space, SMC: smooth muscle cell, SR: sarcoplasmic reticulum, EC: endothelial cell, ER: endoplasmic reticulum, LU: lumen, ECS: extracellular space.

where r_h is the IP_3 production rate and k_{deg} is the degradation rate.

The astrocytic cytosolic Ca^{2+} (Ca_k) comes from both the ER through various channels and from the PVS via the TRPV4 channel:

$$\frac{dCa_k}{dt} = B_{cyt} \left(J_{IP3_k} - J_{pump_k} + J_{ERleak_k} + \frac{J_{TRPV_k}}{r_{buff}} \right) \quad (8)$$

where the flux through the TRPV4 channel (J_{TRPV_k}) is described in Equation (24), and r_{buff} describes the rate of Ca^{2+} buffering at the astrocytic endfoot compared to the main body. Similarly the Ca^{2+} concentration in the astrocytic ER (s_k) is given by

$$\frac{ds_k}{dt} = \frac{-B_{cyt}}{VR_{ERcyt}} (J_{IP3_k} - J_{pump_k} + J_{ERleak_k}) \quad (9)$$

where VR_{ERcyt} is a volume ratio constant. Fast Ca^{2+} buffering is described within the steady state approximation as detailed by Fink et al. (1999):

$$B_{cyt} = \left(1 + BK_{end} + \frac{K_{ex}B_{ex}}{(K_{ex} + Ca_k)^2} \right)^{-1} \quad (10)$$

where BK_{end} is the ratio of the endogenous buffer concentration to the endogenous disassociation constant, K_{ex} is the disassociation constant of exogenous buffer, and B_{ex} is the constant concentration of exogenous buffer.

The ER has 3 mechanisms for Ca^{2+} transport: IP_3R channels that release Ca^{2+} in response to IP_3 , an uptake pump, and a leak channel. The flux of Ca^{2+} through the IP_3R channel is:

$$J_{IP3_k} = J_{max} \left[\left(\frac{i_k}{i_k + K_i} \right) \left(\frac{Ca_k}{Ca_k + K_{act}} \right) h_k \right]^3 \left(1 - \frac{Ca_k}{s_k} \right) \quad (11)$$

where J_{max} is the maximum rate, K_i is the dissociation constant for IP_3R binding, and K_{act} is the dissociation constant for Ca^{2+} binding to an activation site on the IP_3R . The inactivation variable h_k is given by

$$\frac{dh_k}{dt} = k_{on} [K_{inh} - (Ca_k + K_{inh})h_k] \quad (12)$$

where k_{on} and K_{inh} are the Ca^{2+} binding rate and dissociation constant, respectively. The flux of Ca^{2+} through the uptake pump is given by

$$J_{pump_k} = V_{max} \frac{Ca_k^2}{Ca_k^2 + k_{pump}^2} \quad (13)$$

where V_{max} is the maximum pump rate and k_{pump} is the pump constant. The flux of Ca^{2+} through the leak channel is given by

$$J_{ERleak_k} = P_L \left(1 - \frac{Ca_k}{s_k} \right) \quad (14)$$

where P_L is the steady state balance constant.

The ODE for the astrocytic EET concentration (eet_k) is assumed to have the form of

$$\frac{deet_k}{dt} = V_{eet} \max(Ca_k - c_{k_{min}}, 0) - k_{eet} eet_k \quad (15)$$

where V_{eet} is the EET production rate, $c_{k_{min}}$ is the minimum Ca^{2+} concentration required for EET production, and k_{eet} is the decay rate.

3.1.1 BK channel

The following equations are modified from Dormanns et al. (2014) to include astrocytic Ca^{2+} dynamics following the work of Farr and David (2011). Astrocytic Ca^{2+} , EET concentration, and membrane potential v_k all have an opening effect on the astrocytic BK channel on the endfeet adjacent to the PVS. The flux of K^+ through the astrocytic BK channel is given by

$$J_{BK_k} = \frac{g_{BK_k}}{R_k F} w_k (v_k - E_{BK_k}) \quad (16)$$

where g_{BK_k} is the channel conductance per unit area, F is Faraday's constant, and R_k is the astrocytic volume-area ratio (see Dormanns et al. (2014) for further details on this variable). The Nernst potential of the BK channel is given by

$$E_{BK_k} = \frac{R_g T}{z_K F} \ln \left(\frac{K_p}{K_k} \right) \quad (17)$$

where R_g is the universal gas constant, z_K is the ionic valence for K^+ , and K_p and K_k are the perivascular and astrocytic K^+ concentrations respectively (see Dormanns et al. (2014) for further details on these two variables).

The open probability w_k of the voltage, Ca^{2+} and EET mediated BK channel is given by

$$\frac{dw_k}{dt} = \phi_n (w_\infty - w_k) \quad (18)$$

The time constant associated with the opening of the BK channel is given by

$$\phi_n = \psi_n \cosh \left(\frac{v_k - v_3}{2v_4} \right) \quad (19)$$

where ψ_n is the characteristic time constant and v_4 is a measure of the spread of the open probability. The equilibrium state BK channel is written as

$$w_\infty = 0.5 \left(1 + \tanh \left(\frac{v_k + eet_{shift}eet_k - v_3}{v_4} \right) \right) \quad (20)$$

where eet_{shift} determines the EET-dependent shift of the channel. Finally the voltage associated with half open probability is given by

$$v_3 = -\frac{v_5}{2} \tanh \left(\frac{Ca_k - Ca_3}{Ca_4} \right) + v_6 \quad (21)$$

where v_5 , v_6 , Ca_3 and Ca_4 are constants.

The BK channel submodel of Farr and David (2011) used parameters from Gonzalez-Fernandez and Ermentrout (1994), however some of these parameters were more suited to a cell model such as a neuron where the membrane potential depolarises and becomes positive. As such the profile of the steady state open probability w_∞ had a sharp incline between -50 mV and 20 mV (see Figure 3). However in our model the astrocyte only depolarises from -87 mV up to a maximum of -54 mV.

In addition, Cox (2014) modelled a BK channel in the neuron. They found that increasing the Ca^{2+} concentration shifted the profile of the open probability to the left. However, even at very high Ca^{2+} concentrations the open probability was not high unless the cell was depolarised.

Based on the open probability profile at differing Ca^{2+} concentrations in Cox (2014) and the range of v_k that is seen in our model, the parameters of BK channel open probability have been modified (see Figure 3). All parameters in the preceding equations can be found in Table 2 in the Appendix.

3.2 TRPV4 channel

The second extension to the NVU model is a TRPV4 channel on the astrocytic endfoot adjacent to the PVS and is based on the bidirectional model of Witthoft and Karniadakis (2012). In this model vessel dilation activates the TRPV4 channels, allowing an influx of Ca^{2+} from the PVS into the cytosol and hence increasing the astrocytic Ca^{2+} concentration.

The perivascular Ca^{2+} concentration Ca_p is given by

$$\frac{dCa_p}{dt} = -\frac{J_{TRPV_k}}{VR_{pa}} + \frac{J_{VOCC_i}}{VR_{ps}} - Ca_{decay_p}(Ca_p - c_{min_p})$$

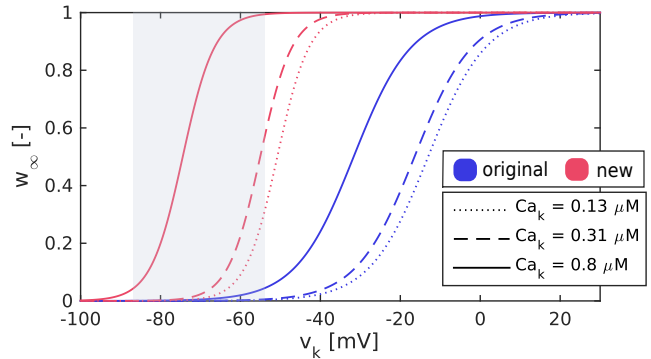


Fig. 3: BK steady state open probability w_∞ varied with astrocytic membrane potential (v_k) at differing astrocytic Ca^{2+} concentration levels (Ca_k), for the original model parameters (blue) and new parameters (red). Grey area: range of v_k in the astrocyte.

$$(22)$$

where VR_{pa} and VR_{ps} are volume ratios, Ca_{decay_p} is the Ca^{2+} decay rate, and c_{min_p} is the resting state equilibrium Ca^{2+} concentration in the PVS. Here J_{VOCC_i} is the flux of Ca^{2+} through the VOCC which connects the SMC to the PVS. When the membrane of the SMC hyperpolarises this channel closes and is given by

$$J_{VOCC_i} = G_{Cai} \frac{v_i - v_{Ca1}}{1 + \exp[-(v_i - v_{Ca2})/R_{Cai}]} \quad (23)$$

where G_{Cai} is the whole cell conductance, v_{Ca1} is the reversal potential, v_{Ca2} is the half point of the VOCC activation sigmoidal, and R_{Cai} is the maximum slope of the activation sigmoidal.

The flux of Ca^{2+} through the TRPV4 channel is given by

$$J_{TRPV_k} = -\frac{G_{TRPV_k}}{2} m_k (v_k - E_{TRPV_k}) \quad (24)$$

where G_{TRPV_k} is the whole cell conductance for TRPV4 channels. The Nernst potential of the TRPV4 channel is given by

$$E_{TRPV_k} = \frac{R_g T}{z_{Ca} F} \log \left(\frac{Ca_p}{Ca_k} \right) \quad (25)$$

where z_{Ca} is the ionic valence for Ca^{2+} .

The open probability of the TRPV4 channel is modelled as an ODE that decays to its equilibrium state m_{∞_k} according to

$$\frac{dm_k}{dt} = \frac{m_{\infty_k} - m_k}{t_{TRPV_k}} \quad (26)$$

where t_{TRPV_k} is the characteristic time constant, and the equilibrium state of the TRPV4 channel is

$$m_{\infty_k} = \Gamma_m \left[\frac{1}{1 + H_{Ca_k}} \left(H_{Ca_k} + \tanh \left(\frac{v_k - v_{1,TRPV}}{v_{2,TRPV}} \right) \right) \right] \quad (27)$$

where $v_{1,TRPV}$ and $v_{2,TRPV}$ are voltage gating constants. The material strain gating term is given by

$$\Gamma_m = \frac{1}{1 + \exp \left(-\frac{\eta - \eta_0}{\kappa_k} \right)} \quad (28)$$

where η_0 is the strain required for half activation and κ_k is a strain constant. The strain on the perivascular endfoot of the astrocyte is taken as approximately equal to local radial strain on the arteriole given that the endfoot surrounds the arteriole, and is given by

$$\eta = \frac{R - R_{passive}}{R_{passive}} \quad (29)$$

where $R_{passive}$ is the resting radius. The Ca^{2+} inhibitory term is given by

$$H_{Ca_k} = \frac{Ca_k}{\gamma_{Cai}} + \frac{Ca_p}{\gamma_{Cae}} \quad (30)$$

where γ_{Cai} and γ_{Cae} are constants associated with intracellular and extracellular Ca^{2+} , respectively.

The astrocytic membrane potential v_k equation is modified from the foundation model to include the TRPV4 channel:

$$v_k = \frac{g_{Na_k} E_{Na_k} + g_{K_k} E_{K_k} + \dots + g_{TRPV_k} m_k E_{TRPV_k}}{g_{Na_k} + g_{K_k} + \dots + g_{TRPV_k} m_k} \quad (31)$$

where g_{TRPV_k} is the TRPV4 channel conductance per unit area (note: not the same as G_{TRPV_k}). The remaining conductances and Nernst potentials are described fully in Dormanns et al. (2014). All relevant parameters in these equations can be found in Table 3 in the Appendix.

3.3 Extracellular space

The NVU model has been extended via the addition of an ECS compartment. Transport of K^+ between the ECS and SC compartments of a single NVU is implemented via a linear diffusion term:

$$J_{diff} = \frac{1}{\tau_s} (K_e - K_s) \quad (32)$$

where J_{diff} is added to or subtracted from the differential equation for the K^+ concentration in the SC (K_s) and the K^+ concentration in the ECS (K_e) respectively. τ_s is the characteristic time in seconds that is needed for K^+ to diffuse over the distance Δx_s :

$$\tau_s = \frac{(\Delta x_s)^2}{2D_K}, \quad D_K = \frac{D_{free}}{\lambda_0^2} \quad (33)$$

Here D_K is the effective diffusion coefficient of K^+ , D_{free} is the diffusion coefficient of K^+ in a free medium, and λ_0 is a non-dimensional tortuosity factor which is necessary because diffusion is hindered by the narrow confines of the ECS (Sykova and Nicholson 2008; Nicholson and Phillips 1981; Nicholson and Sykova 1998).

For diffusion between the ECS and SC, τ_s is based on an average astrocyte length (across two astrocyte arms (Kettenmann and Verkhratsky 2011)) of Δx_s . The ECS is directly connected to the SMC via a Ca^{2+} mediated BK channel and sodium potassium pump (with fluxes denoted by J_K and J_{NaK} respectively) given by:

$$J_K = G_K w_i (v_i - E_K) \quad (34)$$

$$J_{NaK} = F_{NaK} \quad (35)$$

where the G_K is the whole SMC conductance for K^+ efflux, E_K is the BK channel Nernst potential, and F_{NaK} is the rate of K^+ influx into the SMC via the sodium potassium pump. All relevant parameters are detailed in Table 4 in the Appendix. The two variables are w_i , the open state probability of the Ca^{2+} mediated BK channel, and v_i , the SMC membrane potential. These variables are described in detail in Dormanns et al. (2014) and Dormanns et al. (2016). This extension is not the focus of this paper and so no further analysis has been included.

4 Results

4.1 Simulation procedures

A total of 42 coupled ODEs make up the entire single NVU system and are solved in Matlab using the stiff solver ‘ode15s’ due to domains of stiffness encountered in the foundation model of Dormanns et al. (2016). The initial conditions were chosen so that the system is initially at a steady state.

A single NVU is neuronally stimulated via an input of K^+ and glutamate into the SC in order to produce a vascular response through the process of NVC. However with multiple

pathways and components in the NVU the vascular response should vary based on which pathways are active. The effects of each pathway are examined, in particular the contribution of astrocytic Ca^{2+} and the TRPV4 channel. It is important to note that mathematical models are able to shut off or isolate individual pathways which are impossible to do in a wet lab.

The four pathways are activated or deactivated as follows. The K^+ pathway is controlled via the input function $K(t)$ so that when there is no input (i.e. $K_{in} = 0$) the pathway is deactivated. The astrocytic Ca^{2+} pathway is controlled via the input function $Glu(t)$ in a similar manner ($Glu_{max} = 0$). The NO pathway is activated through the input function $Glu(t)$ and deactivated by setting the rates of nNOS and eNOS production to zero, so that no NO can be produced. Finally the TRPV4 channel is deactivated by setting the open probability of the channel to zero so there is no Ca^{2+} flux.

The stimulation input functions are from 100 to 300 s simulation time (indicated by a grey box in the following figures), primarily for the NO pathway as it has a delayed response.

4.2 Astrocytic Ca^{2+} pathway and TRPV4 channel

The effects of the astrocytic Ca^{2+} pathway and the TRPV4 channel implemented in isolation and together are shown in Figure 4.

When only the Ca^{2+} pathway is active, the glutamate release from neuronal stimulation induces a fast release of IP_3 into the astrocyte via metabotropic receptors. Consequently there is an influx of Ca^{2+} into the cytosol through the IP_3 mediated Ca^{2+} channel on the ER. The level of astrocytic Ca^{2+} (Ca_k) increases to $0.31 \mu M$, consistent with the experimental results of Girouard et al. (2010) (see Figure 1). The rise in Ca_k induces an increase in EET concentration (eet_k), and the increase in Ca_k and eet_k both cause a very minor increase in the open probability of the BK channel (w_k). Therefore the flux of K^+ through the BK channel has a corresponding small increase, as does the perivascular K^+ concentration (K_p) and radius of only 0.002% from the baseline. This radial increase is negligible (results not shown).

When the Ca^{2+} pathway is deactivated and the TRPV4 channel active, the TRPV4 channel induces a small constant Ca^{2+}

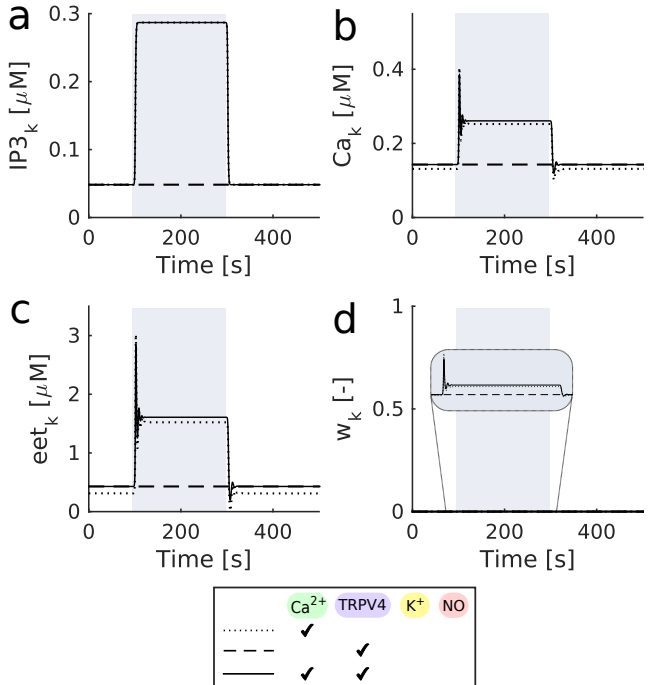


Fig. 4: The effects of the astrocytic Ca^{2+} pathway and TRPV4 channel both individually and together. a) astrocytic IP_3 concentration, b) astrocytic Ca^{2+} concentration, c) astrocytic EET concentration, and d) open probability of the astrocytic BK channel.

flux into the astrocyte which slightly increases the resting Ca_k and eet_k by a small amount. The membrane potential v_k also slightly increases due to the Ca^{2+} ion influx to the cell. This constant Ca^{2+} influx is minor as the TRPV4 channel is stretch dependent and the resting basal radius is small.

The Ca^{2+} pathway and TRPV4 channel together produce the largest increase in w_k , however this increase is still negligible. The increase in w_k is small because the open probability is also strongly voltage dependent (clearly seen in Figure 3), and there is no significant increase in astrocytic membrane potential during stimulation associated with the Ca^{2+} pathway and/or TRPV4 channel. Hence the K^+ flux through the BK channel is not large enough to significantly raise K_p and have any effect on the radius.

4.3 K^+ pathway

The effects of the K^+ pathway with and without the astrocytic Ca^{2+} pathway and TRPV4 channel are shown in Figure 5. The two variable components of the BK flux equation are the open probability w_k and the term $v_k - E_{BK_k}$ (see Equation (16)).

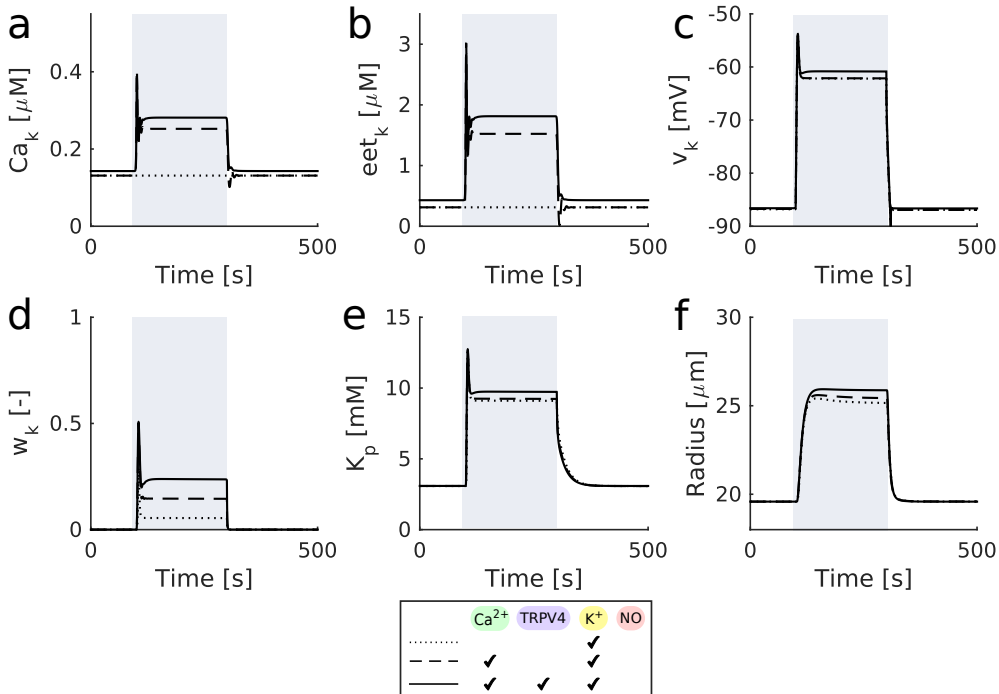


Fig. 5: The effects of the K^+ pathway with the Ca^{2+} pathway and TRPV4 channel. a) astrocytic Ca^{2+} concentration, b) astrocytic EET concentration, c) astrocytic membrane potential, d) open probability of the astrocytic BK channel, e) perivascular K^+ concentration, and f) radius.

When only the K^+ pathway is active, the release of K^+ into the SC is taken up by the astrocyte. This influx of positive ions depolarises the astrocyte and v_k increases. Even though there is no increase in either Ca_k or eet_k , the strong voltage dependency of the BK channel means that w_k increases significantly up to 0.05 and the magnitude of the flux (via the term $v_k - E_{BK_k}$) is large. Consequently the flux through the BK channel is large and K_p increases, leading to a maximal radial increase of 29% from the baseline.

When both the K^+ and Ca^{2+} pathways are active, the increase in Ca_k and eet_k cause w_k to increase up to 0.15, leading to increased K_p and a maximal radial increase of 31% from the baseline. It is important to note that the increase in w_k from the Ca^{2+} pathway is not linearly additive, due to the profile of the steady state open probability w_∞ in Figure 3. By itself the Ca^{2+} pathway is only able to induce a very small increase in w_k , but when the astrocyte is depolarised via the K^+ pathway, Ca^{2+} results in a comparatively large increase in w_k .

When the TRPV4 channel is activated in addition to the K^+ and Ca^{2+} pathways, Ca_k increases further to $0.34 \mu M$. The TRPV4 channel has a larger effect on Ca_k than in the case without K^+ in Figure 4 because of its stretch dependency; when the radius is increased the TRPV4 Ca^{2+} flux also in-

creases, providing a positive feedback loop. The membrane potential v_k slightly increases further due to the influx of positive Ca^{2+} ions through the TRPV4 channel from the PVS into the astrocyte. The increase in Ca_k , eet_k and v_k causes w_k to increase to 0.24 and the magnitude of the BK flux (via term $v_k - E_{BK_k}$) to increase, opening the BK channel further and resulting in an increased maximal radius of 32% of the baseline.

Therefore the Ca^{2+} pathway and TRPV4 channel are able to strengthen NVC induced by the K^+ pathway by increasing the open probability of the BK channel and hence allowing more K^+ into the PVS.

4.4 Nitric oxide pathway

The NO pathway is independent of the dynamics in the astrocyte. When the NO pathway is active, the glutamate release into the SC during neuronal stimulation induces neuronal NO production. The NO from both cells diffuses into the SMC where it increases the production of cGMP and eventually induces vasodilation. The Ca^{2+} pathway and TRPV4 channel have no effect on the NO pathway because they only affect the astrocytic BK channel. Consequently the Ca^{2+}

and TRPV4 channel have a negligible effect as in the case without NO (Figure 4) and do not strengthen NO induced NVC.

4.5 All pathways

The accumulative effects of all four model pathways (K^+ , NO, astrocytic Ca^{2+} , and the TRPV4 channel) on the vascular response are shown in Figure 6. The K^+ pathway has fast radial dynamics that begin 3 seconds after neuronal stimulation begins, reaching the maximal radius in approximately 30 seconds. The radius then slightly decreases before reaching a steady state approximately 100 seconds after stimulation starts. However there is also rapid decay almost directly after stimulation ceases, with the radius reaching the baseline within 30 seconds.

When the NO pathway is active the radial baseline is 23.2 μm , 18% higher due to the vasodilatory effect of the NO continuously produced in the EC. In contrast to the K^+ pathway the dynamics are much slower and the response is delayed. The vascular response to neuronal stimulation begins approximately 8 seconds after stimulation starts. The radius continuously increases at a slow rate until approximately 15 seconds after stimulation has ceased. The radius profile then slowly decays, reaching the baseline after approximately 150 seconds.

When both the K^+ and NO pathways are active the radius experiences a fast initial increase for approximately 30 seconds, before continuously increasing at a slower rate until approximately 5 seconds after stimulation ceases. The radius then slowly decreases back to the baseline over approximately 150 seconds.

When all four components are active (K^+ , NO, Ca^{2+} and TRPV4), the radius increases at a fast rate for approximately 40 seconds, reaching a higher initial maximum than the case without Ca^{2+} and TRPV4. The radius continues to slowly increase and reaches a slightly higher maximal radius approximately 5 seconds after stimulation ceases, and the radius decays to the baseline over 150 seconds. Hence the Ca^{2+} pathway and TRPV4 channel increase the maximal radius of the vascular response due to their effects on the astrocytic BK channel which in turn strengthen the K^+ induced NVC pathway.

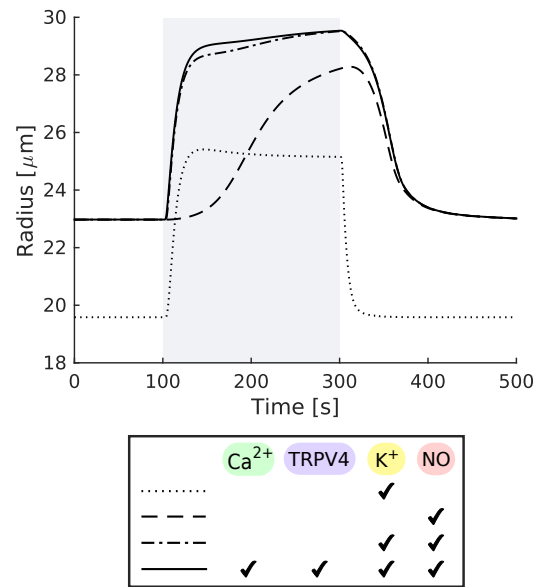


Fig. 6: The effects of both K^+ and NO pathways with the astrocytic Ca^{2+} pathway and TRPV4 channel.

4.6 Ca^{2+} induced vasoconstriction

Various studies have suggested that, in contrast to glutamate induced NVC where a moderate increase in Ca^{2+} concentration can cause vasodilation, larger increases in Ca^{2+} can result in vasoconstriction (Girouard et al. 2010; Dunn et al. 2013; Du et al. 2015). As an example, Du et al. (2015) performed experiments with glutamatergic neurons which exude only glutamate upon activation. They suggest that NO and the neuropeptide vasopressin mediate NVC through different pathways. Vasopressin leads to a rapid and significant increase in astrocytic Ca^{2+} concentration (Zhao and Brinton 2002). According to their data, high concentrations of Ca^{2+} (through the release of vasopressin) results in vasoconstriction, NO causes vasodilation, and when released together there is brief vasodilation followed by constriction.

As Du et al. (2015) studied glutamatergic neurons specifically, the rates of various ion channels and amount of Ca^{2+} released during stimulation may differ from our generic NVU model. To account for this, the maximum rate J_{max} of the IP₃R Ca^{2+} channel on the ER is varied in order to simulate much larger releases of Ca^{2+} from the ER into the astrocyte. However, as shown in Section 4.2, in our model increased Ca^{2+} levels have a negligible effect on the radius without the astrocytic depolarisation caused by the K^+ pathway. In fact, even unphysiologically high Ca^{2+} levels of over 4 μM still have no significant effect (results not shown). Therefore

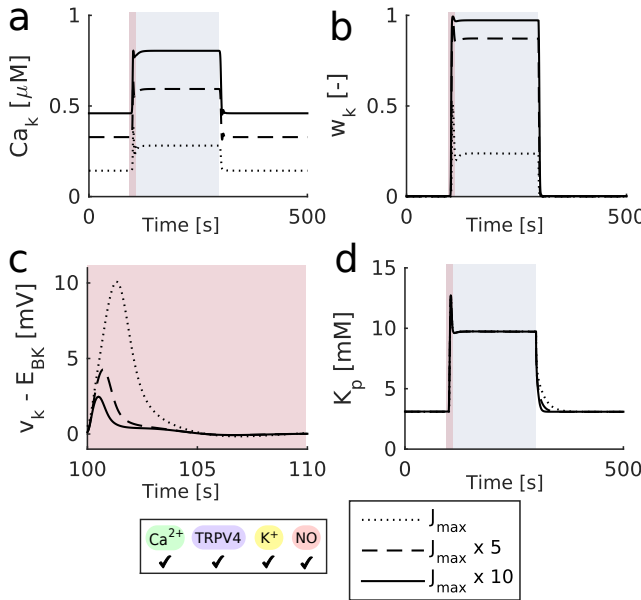


Fig. 7: The effects of high astrocytic Ca^{2+} concentration Ca_k via increased IP_3 induced Ca^{2+} release (J_{max}) in the astrocyte. a) astrocytic Ca^{2+} concentration, b) open probability of the BK channel, c) the component $v_k - E_{BK}$ of the BK flux, and d) the perivascular K^+ concentration.

the effects of high Ca^{2+} are examined with the K^+ pathway active. The behaviour of the NVU in response to high astrocytic Ca^{2+} concentration with all components active is shown in Figure 7.

By increasing J_{max} by a factor of 5, the Ca^{2+} concentration Ca_k during stimulation increases up to $0.6 \mu M$. Whereas increasing J_{max} by a factor of 10 causes Ca_k to increase up to $0.8 \mu M$. This Ca^{2+} concentration is at a similar level to that in the experiment of Girouard et al. (2010) which induced vasoconstriction (see Figure 1). As the astrocyte is depolarised from the K^+ pathway, this high Ca^{2+} level causes the BK channel to almost fully open (w_k almost 1). Consequently the BK flux has a high initial magnitude of K^+ moving into the PVS. But this means that the BK Nernst potential E_{BK} is quick to increase due to the fast increase in perivascular K^+ concentration, so that the term $v_k - E_{BK}$ becomes smaller more quickly. Hence the BK flux will be quick to decrease in magnitude. Conversely, when the open probability is low, the BK flux has a lower initial magnitude and E_{BK} takes longer to increase, so the BK flux will take longer to decrease in magnitude.

Therefore if the channel is only slightly open, the K^+ flux will be of lower magnitude over a longer time, whereas if the channel is almost fully open the K^+ flux will be of higher magnitude over a shorter time. Regardless, over the period

of stimulation the total amount of K^+ through the BK channel will be almost the same, so the effect of increasing w_k is minor. Hence while increasing the Ca^{2+} levels increases the open probability of the BK channel, the effect is counteracted by the fast increase in Nernst potential.

These results show that in our model the only way to significantly increase the amount of K^+ going through the BK channel in order to cause further dilation or vasoconstriction is by increasing the astrocytic membrane potential v_k further; Ca^{2+} is not sufficient. This suggests that either there is some important component missing from the model, or that the increase in Ca^{2+} that occurs at the same time as vasodilation or constriction could simply a by-product of the cell dynamics rather than the source of the vascular response.

5 Discussion and conclusions

The addition of astrocytic Ca^{2+} and the TRPV4 channel to the foundation model of Dormanns et al. (2016) allows for a comparison of the contribution of various different pathways present in the NVU (K^+ , NO, astrocytic Ca^{2+} , and the TRPV4 channel). Changing the BK submodel parameters to fit the astrocyte dynamics rather than neuronal dynamics results in a more physiologically realistic open probability that naturally ranges from 0 to 1 rather than 0 to 0.002.

The K^+ signalling pathway induced by neuronal K^+ release governs the fast onset of vasodilation during neuronal stimulation, while the NO signalling pathway induced by neuronal glutamate release is responsible for maintaining the dilation longer with a slow decline to the basal state following stimulation. The NO produced in the EC increases the basal radius due to constant WSS induced eNOS production.

The TRPV4 channel provides a bidirectional signalling pathway between the astrocyte and the vasculature. The pathway results in an increase in astrocytic Ca^{2+} concentration proportional to the level of vasodilation during neuronal stimulation.

The astrocytic Ca^{2+} pathway induced by glutamate results in a significant increase in the astrocytic Ca^{2+} concentration up to levels consistent with the experimental results of Girouard et al. (2010), but the effect on the astrocytic BK channel (mediated by Ca^{2+} , EET and strongly mediated by membrane potential) is negligible on the basis of

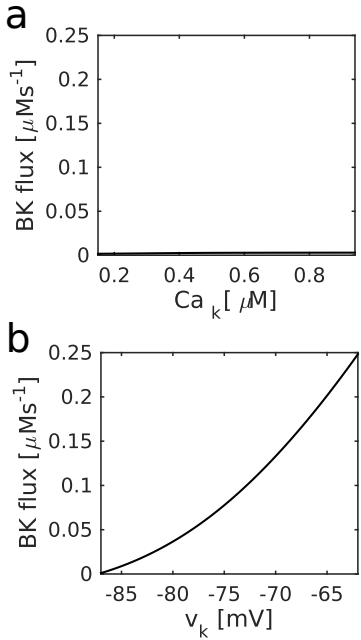


Fig. 8: The effect on the BK flux of a) astrocytic Ca^{2+} (Ca_k) when the astrocytic membrane potential (v_k) is at a constant resting state of -86.5 mV, and b) v_k when Ca_k is at a constant resting state of $0.14 \mu M$.

our model. When the TRPV4 channel is active alongside the Ca^{2+} pathway there is a slight increase in the astrocytic Ca^{2+} concentration, but the effect is minimal as the channel is stretch dependent. Even with an unrealistically high Ca^{2+} concentration, the magnitude of the BK flux is still insignificant to induce either vasodilation or constriction. This is because according to our model the magnitude of the BK flux is strongly dependent on the astrocytic membrane potential, but the membrane potential has little to no change from the Ca^{2+} pathway and TRPV4 channel.

Figure 8 demonstrates how the BK flux changes with both astrocytic Ca^{2+} (Ca_k) and the membrane potential (v_k). Increasing Ca_k from $0.14 \mu M$ up to high concentrations of $0.9 \mu M$ (while keeping v_k at the resting state of -86.5 mV) produces only a very small increase in flux. Whereas increasing v_k from the resting state up to -60 mV (while keeping Ca_k constant at $0.14 \mu M$) produces a large increase in flux. Therefore it is clear that, in our model with astrocytic Ca^{2+} and EET signalling, the astrocyte must depolarise in order for the BK channel flux to increase in magnitude. Hence astrocytic Ca^{2+} with EET signalling does not produce any noticeable vascular response, and on the basis of our model this pathway is insufficient for NVC.

However when the K^+ signalling pathway is active, the release of neuronal K^+ results in astrocytic depolarisation.

Consequently the open probability of the BK channel increases and the magnitude of the BK flux is large (see Figure 8), resulting in vasodilation. When the Ca^{2+} pathway and/or TRPV4 channel are activated alongside the K^+ pathway, the high astrocytic Ca^{2+} and EET concentrations have a noticeable effect on the open probability of the BK channel, opening the channel further and providing a larger flux of K^+ into the PVS. This results in a significant radial increase compared to when only the K^+ pathway is active.

When the astrocytic Ca^{2+} pathway and TRPV4 channel are activated alongside the NO pathway, there is no difference in the vascular response to neuronal stimulation. The Ca^{2+} pathway and TRPV4 channel affect the astrocytic BK channel, but the NO pathway is completely independent of the dynamics in the astrocyte.

In summary, on the basis of our model, by themselves astrocytic Ca^{2+} and EETs have no significant effect on the BK channel and hence no effect on the vasculature. Due to the high dependence of the BK channel on the membrane potential, the astrocyte must depolarise (for example through the K^+ signalling pathway) in order to produce a significant K^+ flux into the PVS and provide a vascular response. Only then can astrocytic Ca^{2+} enhance the vascular response by opening the BK channel further.

While K^+ is a well recognised vasodilator, there is still discussion over the mechanism termed K^+ siphoning which describes the directed release of K^+ from astrocytic endfeet. Metea et al. (2007) produced depolarisations in astrocytes to generate a K^+ efflux from the endfeet, but did not observe any vasodilation. Although it must be noted that these experiments were performed on astrocytes in the retina and not the cortex. Based on the hypothesis that astrocytic KIR channels (not present in our model) provide a substantial role in K^+ siphoning (Kofuji et al. 2000; Butt and Kalsi 2006), Metea et al. (2007) also monitored light activated vascular responses in KIR4.1 knock-out mice. They found that the response was identical in both knock-out and wild-type mice. However, they do not rule out astrocytic BK channels as a valid mechanism for K^+ siphoning.

There are conflicting views on the importance of the astrocytic Ca^{2+} pathway in the literature. Dunn et al. (2013), Girouard et al. (2010) and Filosa et al. (2006) among others claim that Ca^{2+} is an important factor for NVC. However, Gordon et al. (2011) state that there are problems regarding the data interpretation presented by Filosa et al. (2006). One such problem is that the thromboxane A₂ agonist U46619

used in their experiments increases extracellular PgE₂ (Gordon et al. 2008), engaging the prostaglandin pathway and shifting the balance of other pathways to be observed.

In addition, Otsu et al. (2015) using genetically encoded Ca^{2+} sensors in astrocytes examined NVC in the olfactory bulb. Their results indicated only small Ca^{2+} concentrations are seen in the astrocyte and even then are in the processes rather than the astrocyte body. However these increases were extremely small. They observed vasodilation so it may be that these small Ca^{2+} transients come from the stretch dependent TRPV4 channel which are situated on the astrocytic processes. In addition the adult mice that were part of the experiment do not have the mGluR receptor, so IP_3 is most likely unavailable for intracellular Ca^{2+} release. Overall their results seems to suggest that K^+ is the main NVC mechanism. Our results support this; we have shown that while Ca^{2+} is not necessary it does have a strengthening effect on NVC when the K^+ pathway is activated.

One possible reason for the discrepancy in results between our work and experimental data is that, in all papers mentioned prior, the astrocytic K^+ concentration or membrane potential are not explicitly measured. Therefore it is possible that experiments showing vasodilation or vasoconstriction following astrocytic Ca^{2+} increase may be ignoring the contribution of K^+ or the astrocytic membrane potential towards the vascular response. Consequently our results can be considered consistent with those of Girouard et al. (2010) and others as they say nothing about the influence of astrocytic K^+ or membrane potential. This highlights one of the key benefits of mathematical modelling, namely the ability to examine specific components and measure quantities that are difficult or impossible to measure experimentally.

5.1 Limitations and future work

As there are over 60 parameters in the model related to the Ca^{2+} pathway and TRPV4 channel alone, parametric uncertainty is a major limitation. Many of these parameters are models estimations as there is insufficient experimental data available. As such a global parameter sensitivity analysis may be included in future work. Another obvious limitation is the possibility of missing components in the model; two such components are discussed below.

The glutamate induced Ca^{2+} pathway with EET signalling in the astrocyte is shown in our model to be insufficient

for NVC. However, in addition to their effect on the astrocytic BK channel, EETs produced in the astrocyte may also have a direct vasodilatory effect on the SMC (Bennett et al. 2008b; Attwell et al. 2010; Pfister et al. 2010). Astrocytes are also able to produce other vasoactive agents following an increase in Ca^{2+} concentration such as the vasoconstrictor 20-hydroxyeicosatetraenoic acid (20-HETE) and COX derived prostaglandins, which can be either vasodilating or vasoconstricting (Metea and Newman 2006; Mulligan and MacVicar 2004). Bazargani and Attwell (2016) have reviewed astrocytic Ca^{2+} signalling and provide a comprehensive description of Ca^{2+} dynamics. In all three explanatory progressions the assumption is that EETs, prostaglandins and 20-HETE provide the mechanisms for smooth muscle dilation/contraction. However, no explanation is given as to how this works.

Pfister et al. (2010), with their excellent review of vascular pharmacology of EETs, hypothesized that EETs could diffuse to the SMC and activate BK channels leading to K^+ efflux. In turn this would cause hyperpolarisation, closing off the VOCCs and causing relaxation. Fang et al. (1999) indicated that 14,15 EETs increased vascular SMC Ca^{2+} concentration through mediated L-type Ca^{2+} channels via some form of secondary messenger. Ca^{2+} increases caused constriction when the arterial rings were pre-contracted with acetylcholine but relaxed when pretreated with U46619. Although they used human bronchial SMCs, Morin et al. (2007) expressed a second pathway for EETs to relax SMCs. In contrast to the activation of myosin light chain kinase (MLC), this second pathway was possibly due to the activation of protein-kinase C (PKC)-dependent phosphorylation of myosin phosphatase inhibitor protein (CPI-17) to maintain tone, thus assuming that dephosphorylation produced relaxation. Finally we should recognize that EET-induced dynamics resulting in dilation/constriction vary significantly with species and vascular beds.

Further work is required to determine the importance of these vasoactive agents (EETs, 20-HETE, and prostaglandins) and their influence on SMC dynamics; as such they may be included in future version of the model.

As shown in the papers of Hall et al. (2014) and Hill et al. (2015) there is still some controversy concerning the role of arterioles and pericytes in NVC. Fernández-Klett et al. (2010) showed that although pericytes had contractile properties, the main mediation of NVC was arterioles. Using two-photon microscopy they indicated a difference in results

when comparing *in vitro* brain slice experiments with those *in vivo*.

Both *in vitro* and *in vivo* experiments indicate that astrocytes can mediate both dilation and contraction of capillaries (via pericytes) and pre-capillary arterioles. Stobart and Anderson (2013) identified a gliotransmitter pathway using brain slice protocol whereby astrocytes synthesise and release the NMDA receptor agonist D-serine resulting from neuronal activation (although the dilations were small in magnitude). They suggested that dilations could be reduced by inhibition of eNOS and that eNOS and the subsequent production of NO mediated the suppression of 20-HETE. However it is unclear from their experiments as to the influence of astrocytic Ca^{2+} in the dilation of pre-capillary arterioles.

Mishra et al. (2016) provided both *in vitro* and *in vivo* evidence for different pathways for NVC corresponding to either capillary or arteriolar dilations. The astrocytic Ca^{2+} pathway mediated pericyte contraction whilst the NO pathway mediated arteriolar dilation. The Ca^{2+} pathway was not, as is usually assumed, to come from mGluR-5 (which are lacking in mature murine species) but from the activation of the adenosine triphosphate (ATP) receptor P2X1 after release of ATP following neuronal activation. In addition the astrocyte generates AA via phospholipase D2 rather than A2. Finally they indicated that arteriolar dilation depended on NMDA receptor activation and the generation of NO via the Ca^{2+} pathway by interneurons.

On the other hand, by investigating the granular layer of the cerebellum in brain slices, Mapelli et al. (2017) proposed that vasodilation required neuronal NMDA receptors and NOS stimulation followed by guanyl cyclase activation that “probably occurred in pericytes”. Whilst vasoconstriction required metatropic glutamate receptors and the production of 20-HETE. They suggest that there exists a balance between vasoconstricting/dilating systems producing a fine balance of vascular tone. Their introduction plainly stated that pericytes are the major initiator of dilation and referenced both Hall et al. (2014) and Mishra et al. (2016). However the results of Hill et al. (2015) clearly show that there exists no variation in capillary diameter during vasomotion in awake mice. The response of Mishra et al. (2016) to the work of Hill et al. (2015) was to propose a new definition of the pericyte.

Our current model contains only arterioles and no pericytes. The role of pericytes in NVC has not yet been fully deter-

mined with any certainty; further experiments will provide more insight.

6 Acknowledgements

The authors wish to thank the University of Canterbury and Brain Research New Zealand for providing PhD funding for this project.

A Model parameters

All parameters used for the model components discussed in Sections 2 and 3 are given in Tables 1 – 4. See Dormanns et al. (2014, 2016) for the remaining parameters.

References

- Attwell, D., Buchan, A. M., Charpak, S., Lauritzen, M., MacVicar, B. A., and Newman, E. A. (2010). Glial and neuronal control of brain blood flow. *Nature*, 468(7321):232–243.
- Bazargani, N. and Attwell, D. (2016). Astrocyte calcium signaling: the third wave. *Nature neuroscience*, 19(2):182–9.
- Benfenati, V., Amiry-Moghaddam, M., Caprini, M., Mylonakou, M. N., Rapisarda, C., Ottersen, O. P., and Ferroni, S. (2007). Expression and functional characterization of transient receptor potential vanilloid-related channel 4 (TRPV4) in rat cortical astrocytes. *Neuroscience*, 148(4):876–892.
- Bennett, M. R., Farnell, L., and Gibson, W. G. (2008a). A quantitative model of cortical spreading depression due to purinergic and gap-junction transmission in astrocyte networks. *Biophysical journal*, 95(12):5648–5660.
- Bennett, M. R., Farnell, L., and Gibson, W. G. (2008b). Origins of blood volume change due to glutamatergic synaptic activity at astrocytes abutting on arteriolar smooth muscle cells. *Journal of theoretical biology*, 250(1):172–185.
- Bogdanov, V. B., Middleton, N. A., Theriot, J. J., Parker, P. D., Abdullah, O. M., Ju, Y. S., Hartings, J. A., and Brennan, K. C. (2016). Susceptibility of Primary Sensory Cortex to Spreading Depolarizations. *The Journal of Neuroscience*, 36(17):4733–4743.
- Bonder, D. E. and McCarthy, K. D. (2014). Astrocytic Gq-GPCR-linked IP3R-dependent Ca^{2+} signaling does not mediate neurovascular coupling in mouse visual cortex *in vivo*. *Journal of Neuroscience*, 34(39):13139–13150.
- Butt, A. M. and Kalsi, A. (2006). Inwardly rectifying potassium channels (Kir) in central nervous system glia: A special role for Kir4.1 in glial functions. *Journal of Cellular and Molecular Medicine*, 10(1):33–44.
- Cahoy, J. D., Emery, B., Kaushal, A., Foo, L. C., Zamanian, J. L., Christopherson, K. S., Xing, Y., Lubischer, J. L., Krieg, P. A., Krupenko, S. A., Thompson, W. J., and Barres, B. A. (2008). A transcriptome database for astrocytes, neurons, and oligodendrocytes: a new resource for understanding brain development and function. *Journal of Neuroscience*, 28(1):264–278.

- Cao, R. (2011). *The Hemo-Neural Hypothesis: Effects of Vasodilation on Astrocytes in Mammalian Neocortex*. PhD thesis, Massachusetts Institute of Technology.
- Chung, S.-H., Andersen, O. S., and Krishnamurthy, V. V. (2007). *Biological Membrane Ion Channels: Dynamics, Structure, and Applications*. Springer Science & Business Media.
- Cox, D. H. (2014). Modeling a Ca²⁺ channel/BK Ca channel complex at the single-complex level. *Biophysical journal*, 107(12):2797–2814.
- Dormanns, K., Brown, R. G., and David, T. (2016). The role of nitric oxide in neurovascular coupling. *Journal of theoretical biology*, 394:1–17.
- Dormanns, K., van Disseldorp, E. M. J., Brown, R. G., and David, T. (2014). Neurovascular coupling and the influence of luminal agonists via the endothelium. *Journal of theoretical biology*, 364:49–70.
- Drewes, L. R. (2012). Making connexons in the neurovascular unit. *Journal of Cerebral Blood Flow & Metabolism*, 32(8):1455.
- Du, W., Stern, J. E., and Filosa, J. A. (2015). Neuronally-Derived Nitric Oxide and Somatodendritically Released Vasopressin Regulate Neurovascular Coupling in the Rat Hypothalamic Supraoptic Nucleus. *Journal of Neuroscience*, 35(13):5330–5341.
- Dunn, K. M., Hill-Eubanks, D. C., Liedtke, W. B., and Nelson, M. T. (2013). TRPV4 channels stimulate Ca²⁺-induced Ca²⁺ release in astrocytic endfeet and amplify neurovascular coupling responses. *Proceedings of the National Academy of Sciences*, 110(15):6157–6162.
- Fang, X., Weintraub, N. L., Stoll, L. L., and Spector, A. a. (1999). Epoxyeicosatrienoic Acids Increase Intracellular Calcium Concentration in Vascular Smooth Muscle Cells. *Hypertension*, 34(6):1242–1246.
- Farr, H. and David, T. (2011). Models of neurovascular coupling via potassium and EET signalling. *Journal of theoretical biology*, 286(1):13–23.
- Fernández-Klett, F., Offenhauser, N., Dirnagl, U., Priller, J., and Lindauer, U. (2010). Pericytes in capillaries are contractile in vivo, but arterioles mediate functional hyperemia in the mouse brain. *Proceedings of the National Academy of Sciences*, 107(51):22290–22295.
- Filosa, J. A., Bonev, A. D., and Nelson, M. T. (2004). Calcium Dynamics in Cortical Astrocytes and Arterioles During Neurovascular Coupling. *Circulation research*, 95(10):e73–e81.
- Filosa, J. A., Bonev, A. D., Straub, S. V., Meredith, A. L., Wilkerson, M. K., Aldrich, R. W., and Nelson, M. T. (2006). Local potassium signaling couples neuronal activity to vasodilation in the brain. *Nature neuroscience*, 9(11):1397–1403.
- Fink, C. C., Slepchenko, B., and Loew, L. M. (1999). Determination of time-dependent inositol-1,4,5-trisphosphate concentrations during calcium release in a smooth muscle cell. *Biophysical journal*, 77(1):617–628.
- Förstermann, U. (2006). Janus-faced role of endothelial NO synthase in vascular disease: uncoupling of oxygen reduction from NO synthesis and its pharmacological reversal. *Biological chemistry*, 387(12):1521–1533.
- Girouard, H., Bonev, A. D., Hannah, R. M., Meredith, A., Aldrich, R. W., and Nelson, M. T. (2010). Astrocytic endfoot Ca²⁺ and BK channels determine both arteriolar dilation and constriction. *Proceedings of the National Academy of Sciences*, 107(8):3811–3816.
- Girouard, H. and Iadecola, C. (2006). Neurovascular coupling in the normal brain and in hypertension, stroke, and Alzheimer disease. *Journal of applied physiology*, 100(1):328–335.
- Gonzalez-Fernandez, J. M. and Ermentrout, B. (1994). On the origin and dynamics of the vasomotion of small arteries. *Mathematical biosciences*, 119(2):127–167.
- Gordon, G. R. J., Choi, H. B., Rungta, R. L., Ellis-Davies, G. C. R., and MacVicar, B. A. (2008). Brain metabolism dictates the polarity of astrocyte control over arterioles. *Nature*, 456(7223):745–9.
- Gordon, G. R. J., Howarth, C., and MacVicar, B. a. (2011). Bidirectional control of arteriole diameter by astrocytes. *Experimental physiology*, 96(4):393–399.
- Hall, C. N., Reynell, C., Gesslein, B., Hamilton, N. B., Mishra, A., Sutherland, B. A., O'Farrell, F. M., Buchan, A. M., Lauritzen, M., and Attwell, D. (2014). Capillary pericytes regulate cerebral blood flow in health and disease. *Nature*, 508(7494):55–60.
- Hamel, E. (2006). Perivascular nerves and the regulation of cerebrovascular tone. *Journal of applied physiology*, 100(3):1059–1064.
- Higashimori, H., Blanco, V. M., Tuniki, V. R., Falck, J. R., and Filosa, J. A. (2010). Role of epoxyeicosatrienoic acids as autocrine metabolites in glutamate-mediated K⁺ signaling in perivascular astrocytes. *American Journal of Physiology-Cell Physiology*, 299(C1068–C1078.
- Hill, R. A., Tong, L., Yuan, P., Murikinati, S., Gupta, S., and Grutzendler, J. (2015). Regional blood flow in the normal and ischemic brain is controlled by arteriolar smooth muscle cell contractility and not by capillary pericytes. *Neuron*, 87(1):95–110.
- Iadecola, C. (2004). Neurovascular regulation in the normal brain and in Alzheimer's disease. *Nature Reviews Neuroscience*, 5(5):347–360.
- Kettenmann, H. and Verkhratsky, A. (2011). Neuroglia, der lebende Nervenkitt. *Fortschritte der Neurologie-Psychiatrie*, 79(10):588–597.
- Kofuji, P., Ceelen, P., Zahs, K. R., Surbeck, L. W., Lester, H. A., and Newman, E. A. (2000). Genetic Inactivation of an Inwardly Rectifying Potassium Channel (Kir4.1 Subunit) in Mice: Phenotypic Impact in Retina. *J. Neurosci.*, 20(15):5733–5740.
- Lauritzen, M., Dreier, J. P., Fabricius, M., Hartings, J. A., Graf, R., and Strong, A. J. (2011). Clinical relevance of cortical spreading depression in neurological disorders: migraine, malignant stroke, subarachnoid and intracranial hemorrhage, and traumatic brain injury. *Journal of Cerebral Blood Flow & Metabolism*, 31(1):17–35.
- Mapelli, L., Gagliano, G., Soda, T., Laforenza, U., Moccia, F., and D'Angelo, E. U. (2017). Granular layer neurons control cerebellar neurovascular coupling through an NMDA receptor/NO dependent system. *Journal of Neuroscience*, 37(5):1340–1351.
- Metea, M. R., Kofuji, P., and Newman, E. A. (2007). Neurovascular Coupling Is Not Mediated by Potassium Siphoning from Glial Cells. *Journal of Neuroscience*, 27(10):2468–2471.
- Metea, M. R. and Newman, E. A. (2006). Glial cells dilate and constrict blood vessels: a mechanism of neurovascular coupling. *Journal of Neuroscience*, 26(11):2862–2870.
- Mishra, A., Reynolds, J. P., Chen, Y., Gourine, A. V., Rusakov, D. A., and Attwell, D. (2016). Astrocytes mediate neurovascular signaling to capillary pericytes but not to arterioles. *Nature neuroscience*, 19(12):1619–1627.
- Moore, C. I. and Cao, R. (2008). The hemo-neural hypothesis: on the role of blood flow in information processing. *Journal of neurophysiology*, 99(5):2035–2047.

- Morin, C., Sirois, M., Echave, V., Gomes, M. M., and Rousseau, E. (2007). Epoxyeicosatrienoic acid relaxing effects involve Ca²⁺-activated K⁺ channel activation and CPI-17 dephosphorylation in human bronchi. *American Journal of Respiratory Cell and Molecular Biology*, 36(5):633–641.
- Mulligan, S. J. and MacVicar, B. A. (2004). Calcium transients in astrocyte endfeet cause cerebrovascular constrictions. *Nature*, 431(7005):195–199.
- Nakahata, K., Kinoshita, H., Tokinaga, Y., Ishida, Y., Kimoto, Y., Dojo, M., Mizumoto, K., Ogawa, K., and Hatano, Y. (2006). Vasodilation mediated by inward rectifier K⁺ channels in cerebral microvessels of hypertensive and normotensive rats. *Anesthesia & Analgesia*, 102(2):571–576.
- Nicholson, C. and Phillips, J. M. (1981). Ion diffusion modified by tortuosity and volume fraction in the extracellular microenvironment of the rat cerebellum. *The Journal of Physiology*, 321:225–257.
- Nicholson, C. and Sykova, E. (1998). Extracellular space structure revealed by diffusion analysis. *Trends in neurosciences*, 21(5):207–215.
- Nizar, K., Uhlirova, H., Tian, P., Saisan, P. A., Cheng, Q., Reznichenko, L., Weldy, K. L., Steed, T. C., Sridhar, V. B., MacDonald, C. L., Cui, J., Gratiy, S. L., Sakadzic, S., Boas, D. A., Beka, T. I., Einevoll, G. T., Chen, J., Masliah, E., Dale, A. M., Silva, G. A., and Devor, A. (2013). In vivo Stimulus-Induced Vasodilation Occurs without IP₃ Receptor Activation and May Precede Astrocytic Calcium Increase. *Journal of Neuroscience*, 33(19):8411–8422.
- Otsu, Y., Couchman, K., Lyons, D. G., Collot, M., Agarwal, A., Mallet, J.-m., Pfrieger, F. W., Bergles, D. E., and Charpak, S. (2015). Calcium dynamics in astrocyte processes during neurovascular coupling. *Nature neuroscience*, 18(2):210–218.
- Pfister, S. L., Gauthier, K. M., and Campbell, W. B. (2010). Vascular Pharmacology of Epoxyeicosatrienoic Acids. *Advances in Pharmacology*, 60:27–59.
- Pietrobon, D. and Moskowitz, M. A. (2014). Chaos and commotion in the wake of cortical spreading depression and spreading depolarizations. *Nature Reviews Neuroscience*, 15(6):379–393.
- Stobart, J. L. and Anderson, C. M. (2013). Multifunctional role of astrocytes as gatekeepers of neuronal energy supply. *Frontiers in Cellular Neuroscience*, 7:38.
- Straub, S. V., Bonev, A. D., Wilkerson, M. K., and Nelson, M. T. (2006). Dynamic inositol trisphosphate-mediated calcium signals within astrocytic endfeet underlie vasodilation of cerebral arterioles. *The Journal of general physiology*, 128(6):659–669.
- Sykova, E. and Nicholson, C. (2008). Diffusion in brain extracellular space. *Physiological reviews*, 88(4):1277–1340.
- Takata, N., Nagai, T., Ozawa, K., Oe, Y., Mikoshiba, K., and Hirase, H. (2013). Cerebral Blood Flow Modulation by Basal Forebrain or Whisker Stimulation Can Occur Independently of Large Cytosolic Ca²⁺ Signaling in Astrocytes. *PloS one*, 8(6):e66525.
- Witthoft, A., Filosa, J. A., and Karniadakis, G. E. (2013). Potassium buffering in the neurovascular unit: models and sensitivity analysis. *Biophysical Journal*, 105(9):2046–2054.
- Witthoft, A. and Karniadakis, G. E. (2012). A bidirectional model for communication in the neurovascular unit. *Journal of theoretical biology*, 311:80–93.
- Zhao, L. and Brinton, R. D. (2002). Vasopressin-induced cytoplasmic and nuclear calcium signaling in cultured cortical astrocytes. *Brain research*, 943(1):117–131.
- Zonta, M., Angulo, M. C., Gobbo, S., Rosengarten, B., Hossmann, K.-A., Pozzan, T., and Carmignoto, G. (2003). Neuron-to-Astrocyte signaling is central to the dynamic control of brain microcirculation. *Nature neuroscience*, 6(1):43–50.

Parameter	Value	Unit	Description
t_0	100	s	Start time of neuronal stimulation
t_1	300	s	End time of neuronal stimulation
t_β	1	s	Time constant for $K(t)$
α_n	2	[\cdot]	Beta distribution constant for $K(t)$ (Dormanns et al. 2014)
β_n	5	[\cdot]	Beta distribution constant for $K(t)$ (Dormanns et al. 2014)
K_{in}	1.84×10^{-4}	$\mu\text{M m s}^{-1}$	Scaling factor for $K(t)$ (Dormanns et al. 2014)
Δt	10	s	Duration of initial input for $K(t)$
Glu_{\max}	1846	μM	Glutamate release from one vesicle (Dormanns et al. 2016)
θ_L	1	s	Slope scaling factor for $\text{Glu}(t)$ (M.E.) ¹
θ_R	1	s	Slope scaling factor for $\text{Glu}(t)$ (M.E.)

Table 1: Model parameters related to the neuronal input functions $K(t)$ and $\text{Glu}(t)$. ¹Model estimation.

Parameter	Value	Unit	Description
ρ_{\min}	0.1	[\cdot]	Minimum ratio of bound to unbound IP_3 receptors (Farr and David 2011)
ρ_{\max}	0.7	[\cdot]	Maximum ratio of bound to unbound IP_3 receptors (Farr and David 2011)
δ	1.235×10^{-2}	[\cdot]	Ratio of the activities of the unbound and bound receptors (Farr and David 2011)
K_G	8.82	[\cdot]	G-protein disassociation constant (Farr and David 2011)
r_h	4.8	$\mu\text{M s}^{-1}$	Maximum rate of IP_3 production in astrocyte due to glutamate receptors (Farr and David 2011)
k_{deg}	1.25	s^{-1}	Rate constant for IP_3 degradation in astrocyte (Farr and David 2011)
r_{buf}	0.05	[\cdot]	Rate of Ca^{2+} buffering at the endfoot compared to the astrocyte body (M.E.)
VR_{ERcyt}	0.185	[\cdot]	Volume ratio between ER and astrocytic cytosol (Farr and David 2011)
BK_{end}	40	[\cdot]	Ratio of endogenous buffer concentration to disassociation constant (Fink et al. 1999)
K_{ex}	0.26	μM	Disassociation constant of exogenous buffer (Fink et al. 1999)
B_{ex}	11.35	μM	Concentration of exogenous buffer (Fink et al. 1999)
J_{\max}	2880	$\mu\text{M s}^{-1}$	Maximum rate of Ca^{2+} through the IP_3 mediated channel (Farr and David 2011)
K_i	0.03	μM	Disassociation constant for IP_3 binding to an IP_3R (Farr and David 2011)
K_{act}	0.17	μM	Disassociation constant for Ca^{2+} binding to an activation site on an IP_3R (Farr and David 2011)
k_{on}	2	$\mu\text{M}^{-1} \text{s}^{-1}$	Rate of Ca^{2+} binding to the inhibitory site on the IP_3R (Farr and David 2011)
K_{inh}	0.1	μM	Disassociation constant of IP_3R (Farr and David 2011)
V_{\max}	20	$\mu\text{M s}^{-1}$	Maximum rate of Ca^{2+} uptake pump on the ER (Farr and David 2011)
k_{pump}	0.24	μM	Ca^{2+} uptake pump disassociation constant (Farr and David 2011)
P_L	0.0804	$\mu\text{M s}^{-1}$	ER leak channel steady state balance constant (Farr and David 2011)
V_{eet}	72	s^{-1}	EET production rate (Farr and David 2011)
$c_{k_{min}}$	0.1	μM	Minimum Ca^{2+} concentration required for EET production (Farr and David 2011)
k_{eet}	7.2	s^{-1}	EET degradation rate (Farr and David 2011)
g_{BK_k}	6.08×10^{-2}	S m^{-2}	BK channel conductance per unit area (Filosa et al. 2006)
F	96.5	$\text{J mV}^{-1} \text{ mol}^{-1}$	Faraday's constant
R_g	8.315	$\text{J mol}^{-1} \text{ K}^{-1}$	Universal gas constant
z_K	1	[\cdot]	Ionic valence for K^+
ψ_n	2.664	s^{-1}	Characteristic time for the opening of the BK channel (Dormanns et al. 2014)
v_4	8	mV	Measure of the spread of w_∞ (M.E.)
eet_{shift}	2	$\text{mV } \mu\text{M}^{-1}$	Describes the EET dependent voltage shift (Farr and David 2011)
v_5	15	mV	Determines the range of the shift of w_∞ as Ca^{2+} varies (M.E.)
v_6	-55	mV	Shifts the range of w_∞ (M.E.)
Ca_3	0.4	μM	BK open probability Ca^{2+} constant (Farr and David 2011)
Ca_4	0.35	μM	BK open probability Ca^{2+} constant (Farr and David 2011)

Table 2: Model parameters related to the astrocytic Ca^{2+} pathway.

Parameter	Value	Unit	Description
VR_{pa}	0.001	[\cdot]	Volume ratio between PVS and astrocyte (Dormanns et al. 2014)
VR_{ps}	0.001	[\cdot]	Volume ratio between PVS and SMC (Dormanns et al. 2014)
Ca_{decay_p}	0.5	s^{-1}	Rate of decay of Ca^{2+} in PVS (Witthoft and Karniadakis 2012)
c_{min_p}	2000	μM	steady state value of Ca^{2+} in PVS (Witthoft and Karniadakis 2012)
G_{Cai}	1.29×10^{-3}	$\mu M\ mV^{-1}\ s^{-1}$	VOCC whole cell conductance (Dormanns et al. 2014)
v_{Ca1}	100	mV	VOCC reversal potential (Dormanns et al. 2014)
v_{Ca2}	-24	mV	Half point of the VOCC activation sigmoidal (Dormanns et al. 2014)
R_{Cai}	8.5	mV	Maximum slope of the VOCC activation sigmoidal (Dormanns et al. 2014)
G_{TRPV_k}	1.5×10^{-3}	$\mu M\ mV^{-1}\ s^{-1}$	TRPV4 whole cell conductance (Witthoft et al. 2013)
z_{Ca}	2	[\cdot]	Ionic valence for Ca^{2+}
t_{TRPV_k}	0.9	s	Characteristic time constant for m_k (Witthoft and Karniadakis 2012)
η_0	0.1	[\cdot]	Strain required for half activation of the TRPV4 channel (Witthoft and Karniadakis 2012)
κ_k	0.1	[\cdot]	TRPV4 channel strain constant (Witthoft and Karniadakis 2012)
$R_{passive}$	20	μm	Vessel radius when passive and no stress is applied (Dormanns et al. 2014)
$v_{1,TRPV}$	120	mV	TRPV4 channel voltage gating constant (Witthoft and Karniadakis 2012)
$v_{2,TRPV}$	13	mV	TRPV4 channel voltage gating constant (Witthoft and Karniadakis 2012)
γ_{Cai}	0.01	μM	Ca^{2+} concentration constant (Witthoft and Karniadakis 2012)
γ_{Cae}	200	μM	Ca^{2+} concentration constant (Witthoft and Karniadakis 2012)
g_{TRPV_k}	1.35×10^{-2}	$S\ m^2$	TRPV4 channel conductance per unit area (Witthoft et al. 2013)

Table 3: Model parameters related to the TRPV4 channel.

Parameter	Value	Unit	Description
D_{free}	4.58×10^{-9}	$m^2\ s^{-1}$	K^+ diffusion coefficient in a free medium (Sykova and Nicholson 2008)
γ_0	1.6	[\cdot]	Non dimensional tortuosity factor (Nicholson and Phillips 1981)
Δx_s	1×10^{-4}	m	Average distance across two astrocyte arms (Kettenmann and Verkhratsky 2011)
τ_s	2.8	s	Characteristic time for diffusion between the SC and ECS
G_K	4.46×10^{-3}	$\mu M\ mV^{-1}\ s^{-1}$	Whole SMC conductance for K^+ efflux (Dormanns et al. 2014)
E_K	-94	mV	Nernst potential for the SMC BK channel (Dormanns et al. 2014)
F_{NaK}	4.32×10^{-2}	$\mu M\ s^{-1}$	Rate of K^+ influx by the sodium potassium pump (Dormanns et al. 2014)

Table 4: Model parameters related to the ECS compartment.